

adversarially trained models.

2. RELATED WORK

2.1. Adversarial attacks

Denote the original images as x^{real} and the adversarial examples as x^{adv} . Besides, we let \mathcal{F} represents the set of all image classifiers and $\mathcal{F}_t \subset \mathcal{F}$ represents the set of surrogate models. Meanwhile, we use $f(\cdot)$ to denote the classifiers and the L to denote the corresponding loss function (e.g. cross-entropy loss). Crafting adversarial examples could be formalized as an optimization problem:

$$\arg \max_{x^{adv}} \mathbb{E}_{f \in \mathcal{F}} L(f(x^{adv}), y), s.t. \|x^{adv} - x^{real}\|_{\infty} \leq \epsilon. \quad (1)$$

However, in real scenarios, attackers usually could not access the deployed model in \mathcal{F} . An alternative solution is to craft adversarial examples on surrogate models \mathcal{F}_t , and transfer them to target models.

2.2. Transfer attacks

Due to its effectiveness and simplicity, transfer attacks have garnered significant attention. Several methods have been devised to enhance transferability, and we classify them into three categories.

Gradient-based Methods: Drawing an analogy to the optimization and regularization in neural network training, [4] proposed the Momentum Iterative (MI) method and [10] proposed the Nesterov Iterative (NI) method, which introduce the momentum and the Nesterov accelerated gradient to prevent the adversarial examples from falling into the undesired local optima. [7] proposed the variance tuning (VMI) to reduce the variance of the gradient and tuning the current gradient with the gradient variance in the neighborhood of the previous data point.

Input Transformations: Analogous to the data augmentation, [6] proposed the Diverse Inputs (DI) method by applying random transformations to the input images at each iteration. [5] proposed Translation-Invariant (TI) method by optimizing a perturbation over an ensemble of translated images.

Ensemble Attacks: [11] draw an analogy between the number of classifiers used in crafting adversarial examples and the size of training sets in neural network training, argue that increasing the surrogate models could reduce the generalization error upper bound. [8] introduce the SVRG optimizer into ensemble attack to reduce the variance of the gradients during optimization. [9] proposed the common weakness of the ensemble models by showing that both the flatness of loss landscape and the distance between the local optimums

Algorithm 1: ST attacker

```

1 Require: natural image  $x^{real}$ , label  $y$ , loss function
   $L$ , surrogate models  $\mathcal{F}_t = \{f_i\}_i^n$ , perturbation
  budget  $\epsilon$ , iterations  $T$ , learning rate  $\beta$ , loss weight
   $\lambda_1$ , cosine weight  $\lambda_2$ .
2 for  $t = 0 : T - 1$  do
3   Initialize:  $x_0 = x^{real}$ ;
4   for  $i = 1 : n$  do
5     Calculate  $g_{i-1} = \nabla_x L(f_i(x_t^{i-1}), y)$ ;
6     Update adversarial sample by
        $x_t^i = clip_{x^{real}, \epsilon}(x_t^{i-1} + \beta \cdot \frac{g_{i-1}}{\|g_{i-1}\|_2})$ 
7   end
8   Calculate  $g_{mean} = \frac{1}{n} \sum_i \frac{\nabla_x L(f_i(x_t), y)}{\|\nabla_x L(f_i(x_t), y)\|_2}$ ;
9    $diff = x_t^{new} - x_t$ ,  $g_{cos} = diff - g_{mean}$ ;
10  Calculate  $g_{whole} = \lambda_1 g_{mean} + \lambda_2 g_{cos}$ ;
11  Update  $x_{t+1} = clip_{x^{real}, \epsilon}(x_t + g_{whole})$ 
12 end
Result:  $x_T$ 

```

are strongly correlated with the transferability, and the cosine similarity between gradients are upper bound of the latter term. However, the algorithms in [9] are limited. First, their algorithms are ineffective because their methods has to promote the cosine similarity between gradients and loss with a fixed ratio $1 : \frac{\beta}{2}$. Besides, the interplay between loss and cosine similarity, which correspond to the optimization and regularization, remains inadequately explored.

3. METHODOLOGY

3.1. Cosine similarity between gradients

We use p_i to denote the closest optimum of the i th model $f_i \in \mathcal{F}$ to the adversarial example x and use H_i to denote the Hessian matrix of $L(f_i(x), y)$ at p_i . We employ the second-order Taylor expansion to approximate Eq. (1) at p_i :

$$\mathbb{E}_{f_i \in \mathcal{F}} [L(f_i(p_i), y) + \frac{1}{2}(x - p_i)^T H_i(x - p_i)] \quad (2)$$

According to Eq. (2), we can find that a larger value of $\mathbb{E}[L(f_i(p_i), y)]$ and $\mathbb{E}[(x - p_i)^T H_i(x - p_i)]$ means a better performance. For the first term, [12, 13] have proven that the local optima have nearly the same value with the global optimum in neural networks. Therefore, we mainly focus on the second term to improve the transferability of adversarial examples.

[9] use the Cauchy-Swartz theorem and get the upper bound of the second term as:

$$\mathbb{E}[(x - p_i)^T H_i(x - p_i)] \leq \mathbb{E}[\|H_i\|_F] \mathbb{E}[\|(x - p_i)\|_2^2]. \quad (3)$$

The first term correspond to the flatness of the landscape, which is a crucial factor for the generalization ability [14–16].

Method	AlexNet	VGG16	GoogLeNet	InceptionV3	ResNet152	DenseNet121	SqueezeNet	ShuffleNetV2	MobileNetV3	EfficientNetB0	MNASNet	RegNetX400MF	ConvNeXt	ViT-B/16	Swin-S	MaxViT
FGSM	76.4	68.9	54.4	54.5	54.5	57.4	85.0	81.2	58.9	50.8	64.1	57.1	39.8	33.8	34.0	31.3
BIM	54.9	86.1	76.6	64.9	96.0	93.0	80.4	65.3	55.6	80.2	80.8	81.1	68.6	35.0	48.2	49.7
MI	73.2	91.9	89.1	84.6	96.6	95.8	89.4	79.9	71.8	90.1	88.8	89.3	81.6	59.2	66.0	66.1
DI-MI	78.9	92.9	92.0	89.0	93.8	93.8	92.9	85.7	78.6	91.5	91.5	91.2	85.4	66.8	74.2	73.2
TI-MI	78.0	82.5	77.8	75.7	87.8	88.0	85.8	78.2	74.5	76.8	75.5	82.4	56.2	56.9	40.9	32.7
VMI	83.3	94.8	94.2	91.1	97.1	96.6	94.2	89.9	87.3	94.6	94.1	95.3	92.4	81.8	84.2	83.5
MI-SVRG	82.5	96.4	95.7	92.6	99.0	99.1	96.1	90.3	80.6	96.7	94.2	95.4	88.2	65.8	73.4	71.1
MI-SAM	81.0	95.6	94.4	89.2	97.9	98.0	94.1	87.9	80.7	95.2	94.3	93.9	90.1	68.9	75.1	75.6
MI-CSE	93.6	99.6	98.8	97.3	99.9	99.9	99.1	97.2	94.6	98.8	99.1	98.9	96.2	89.6	88.6	85.8
MI-CWA	94.6	99.5	99.0	97.2	99.8	99.8	99.3	97.3	95.7	98.9	98.7	99.4	95.4	89.6	87.6	85.9
MI-ST	94.2	99.7	99.1	97.1	100.0	100.0	99.0	96.9	95.2	99.3	98.9	98.9	96.5	90.6	88.5	86.9

Table 1. Black-box attack success rate(%, \uparrow) on NIPS2017 dataset. Our method performs well on 16 normally trained models with various architectures.

Method	FGSMAT	EnsAT	FastAT	PGDAT	PGDAT	PGDAT	PGDAT [†]	PGDAT [†]
Backbone	InceptionV3	IncResV2	ResNet50	ResNet50	ResNet18	WRN50-2	XCiT-M	XCiT-L
FGSM	53.9	32.5	45.6	36.3	46.8	27.7	23.0	19.8
BIM	43.4	28.5	41.6	30.9	41.0	20.9	16.4	15.7
MI	55.9	42.5	45.7	37.4	45.7	27.8	22.8	19.8
DI-MI	61.8	52.9	47.1	38.0	47.7	31.3	25.4	21.7
TI-MI	66.1	58.5	49.3	43.9	50.7	37.0	29.4	26.9
VMI	72.3	66.4	51.4	47.1	48.9	36.2	33.4	30.8
MI-SVRG	66.8	46.8	51.0	43.9	48.5	33.0	30.2	26.7
MI-SAM	64.5	47.9	50.6	43.9	48.0	33.4	31.8	26.9
MI-CSE	89.6	78.2	75.0	73.5	68.4	64.4	77.5	71.0
MI-CWA	89.6	79.1	74.6	73.6	69.5	64.8	77.8	71.7
MI-ST	90.0	81.4	75.8	75.1	69.7	65.1	78.4	72.2

Table 2. Black-box attack success rate(%, \uparrow). Our method leads the performance on 8 adversarially trained models available on RobustBench. Note that PGDAT[†] is a variant of PGDAT tuned by bag of tricks. It turns out that our method improve the transferability of the adversarial examples.

And has been adequately explored in [14]. In this work, we mainly focus on $\mathbb{E}[\|(x - p_i)\|_2^2]$. Since it's hard to directly optimize $\frac{1}{n} \sum_{i=1}^n \|x - p_i\|_2^2$, [9] derives an upper bound:

$$\frac{1}{n} \sum_{i=1}^n \|x - p_i\|_2^2 \leq -\frac{2 \max \|H_i^{-1}\|_F^2}{n} \sum_{i=1}^n \sum_{j=1}^{i-1} g_i g_j, \quad (4)$$

Where g_i is the loss gradient of the surrogate model i . Consequently, we find that maximizing the cosine similarity between gradients will result in a better generalization ability.

3.2. Derivation of ST

However, the cosine similarity between gradients is still hard to optimize. To this end, [9] proposes an approximation algorithm named MI-CSE, which first update x_i with the current gradient $g_{i-1} = \nabla_x L(f_i(x_{i-1}, y))$ in the inner optimization:

$$x_t^i = \text{clip}_{x^{\text{real}}, \epsilon}(x_t^{i-1} + \beta \frac{g_{i-1}}{\|g_{i-1}\|_2}) \quad (5)$$

And view the update $x_t^n - x_t$ as the approximated gradient for iteration t :

$$x_{t+1} = \text{clip}_{x^{\text{real}}, \epsilon}(x_t + \alpha \cdot \text{sign}(x_t^n - x_t)) \quad (6)$$

It has been proven that updating using such algorithm equivalent to maximizing the cosine similarity between gra-

dients and the loss function simultaneously:

$$\mathbb{E}[x_t^n - x_t] \approx \beta \mathbb{E}[\sum_{i=1}^n \frac{g_i}{\|g_i\|_2}] + \frac{\beta^2}{2} \mathbb{E}[\sum_{i < j} \frac{\partial \frac{g_i g_j}{\|g_i\|_2 \|g_j\|_2}}{\partial x}] \quad (7)$$

However, the proportion of weights of the $\mathbb{E}[\sum_{i=1}^n \frac{g_i}{\|g_i\|_2}]$ and $\mathbb{E}[\sum_{i < j} \frac{\partial \frac{g_i g_j}{\|g_i\|_2 \|g_j\|_2}}{\partial x}]$ are limited to $1 : \frac{\beta}{2}$, making it hard to trade-off between optimization and regularization. Besides, this algorithm has $O(\beta^3)$ approximation error, increasing β will cause a larger approximation error, leading to performance degradation.

In order to get away from the constraints, we find that we could first accurately calculate $g_{\text{loss}} = \sum_{i=1}^n \frac{g_i g_j}{\|g_i\|_2 \|g_j\|_2}$ directly, and we use the update $x_t^n - x_t$ minus the loss term to get the cosine term $g_{\text{cos}} = \sum_{i < j} \frac{\partial \frac{g_i g_j}{\|g_i\|_2 \|g_j\|_2}}{\partial x}$. Finally, we combine them to update as follows:

$$\mathbb{E}[x_t^n - x_t] = \lambda_1 g_{\text{loss}} + \lambda_2 g_{\text{cos}} \quad (8)$$

Which gives us more flexibility to trade-off between optimization and regularization.

3.3. Incorporation with previous attackers

As shown in Algorithm 1, our method could be view as first calculating the update $g_{\text{whole}} = \lambda_1 g_{\text{loss}} + \lambda_2 g_{\text{cos}}$ and then perform gradient ascent. Since our method are orthogonal to input transformation methods like DI [6], TI [5], it can be incorporated with them seamlessly to achieve improved performance. For gradient-based method, like MI [4], NI [10] and VMI [7], we could directly view g_{whole} as current gradients and calculating the corresponding momentums. Hence, our method is easy to be combined with other previous works to further improve the transferability.

4. EXPERIMENT

4.1. Experiment settings

We adopt exactly the same settings as [9]. **Dataset:** We use the NIPS2017 dataset, which is comprised of 1000 images selected from ImageNet. All the images are resized

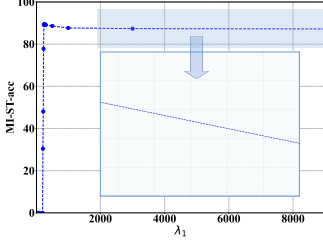


Fig. 1. Loss weight λ_1

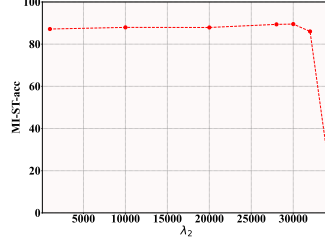


Fig. 2. Cosine weight λ_2

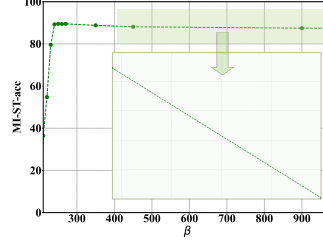


Fig. 3. Inner step size β

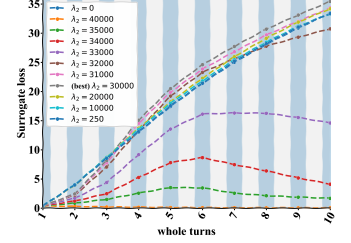


Fig. 4. Gap between λ_1 and λ_2

to 224×224 . **Surrogate Models:** We choose four normally trained models, ResNet18, ResNet32, ResNet50, and ResNet101 from TorchVision [17] and two adversarially trained models, ResNet50 [18] and XCI-T-S12 [19] from [20], which is effective to assess the method’s ability to utilize diverse surrogate models. **Black-box Models:** We evaluate the attack success rate on 24 black-box models, including 16 normally trained models with different architectures and 8 adversarially trained models from RobustBench. **Compared Method:** We compare our methods with FGSM [2], BIM [21], MI [4], DI [6], TI [5], VMI [7], SVRG [8], SAM [9], CSE [9], CWA [9]. **Hyper-parameters:** We set the hyper-parameters as: perturbation threshold $\epsilon = 16/255$, total iteration rounds $T = 10$, momentum decay rate $\mu = 1$, learning rate $\beta = 250$, $r = 16/255/15$, $\alpha = 16/255/5$.

4.2. Adversarial attacks on state-of-the-art models

Attacks on Discriminative Classifiers: As shown in Table 1, MI-ST achieves more than 80% attack success rate over all target models, indicating that even the state-of-the-art classifiers could be easily attacked in black-box setting. Besides, for models resembling any of the surrogate models, MI-ST results in a higher attack success rate. This could be attributed to MI-ST’s encouragement of cosine similarity between gradients, effectively enhancing the optimization across all surrogate models simultaneously. For other models, MI-ST exhibits an improvement of at least approximately 20%, highlighting the strong generalization ability of our approach.

Attacks on Secured Models: As shown in Table 2, among all target models, MI-ST demonstrates an improvement of at least 30% over MI. Moreover, MI-ST surpasses the attack success rates of all preceding algorithms. These results demonstrate the strong effectiveness of MI-ST even against the most formidable defenses, underscoring the threat posed to deployed deep learning models by potential attacks.

4.3. Ablation studies

The gradient of the loss, controlled by λ_1 , primarily governs the optimization of the loss function. Meanwhile, the gradient of the cosine term, governed by λ_2 , play a crucial role in regularization and generalization. Therefore, we ought to

carefully tradeoff between these two terms.

Loss weight λ_1 : As shown in Fig. 1, an increase in λ_1 weakens the impact of the regularization, resulting in a slight decline in attack success rate. We also observe that the attack success rate of models that are not similar to the surrogate models drops significantly. This shows the regularization ability of cosine similarity between gradients, especially for models that are not similar to surrogate models. On the other hand, a too small λ_1 will leading to insufficient optimization of loss functions over the surrogate models, thus leading to a decline in the attack success rate.

Cosine weight λ_2 : To further understand the impact towards optimization, we visualize the average losses over surrogate models with respect to λ_2 and T in Fig. 4. As shown, an excessively large λ_2 significantly impacts optimization, making it hard to maximize the loss function, resulting in degradation of the attack success rate for both surrogate and target models. Furthermore, as observed in Fig. 2, when λ_2 gradually decreases, the regularization effect gradually diminishes, leading to a gradual reduction in transferability.

Inner step size β : Based on Fig. 3, an increase in β leads to a larger error term in the Taylor expansion, resulting in a slight decrease in the attack success rate. This decline is more notable for defense models, as attacking such models demands more precise gradients. However, excessively reducing β can cause our model to converge into local optima and lead to insufficient optimization, significantly impacting the attack success rate.

5. CONCLUSION

In this paper, we propose MI-ST to boost adversarial attacks by promoting cosine similarity between the gradients of each model. We conduct extensive experiments to validate the effectiveness of the proposed methods and explain why they work in practice. To further improve the transferability of the generated adversarial examples, we did extensive experiments to find the best trade-off between optimization and regularization. Among 24 discriminative classifiers and defended models, our method outperforms state-of-the-art attackers on 18 of them. The results identify the vulnerability of the current defenses, and raise security issues for the development of more robust deep learning models.

6. REFERENCES

- [1] Nicholas Carlini and David Wagner, “Towards evaluating the robustness of neural networks,” in *2017 IEEE Symposium on Security and Privacy (SP)*, 2017, pp. 39–57.
- [2] Ian J Goodfellow, Jonathon Shlens, and Christian Szegedy, “Explaining and harnessing adversarial examples,” *arXiv preprint arXiv:1412.6572*, 2014.
- [3] Yanpei Liu, Xinyun Chen, Chang Liu, and Dawn Song, “Delving into transferable adversarial examples and black-box attacks,” *arXiv preprint arXiv:1611.02770*, 2016.
- [4] Yinpeng Dong, Fangzhou Liao, Tianyu Pang, Hang Su, Jun Zhu, Xiaolin Hu, and Jianguo Li, “Boosting adversarial attacks with momentum,” in *Proceedings of the IEEE conference on computer vision and pattern recognition*, 2018, pp. 9185–9193.
- [5] Yinpeng Dong, Tianyu Pang, Hang Su, and Jun Zhu, “Evading defenses to transferable adversarial examples by translation-invariant attacks,” in *Proceedings of the IEEE/CVF Conference on Computer Vision and Pattern Recognition*, 2019, pp. 4312–4321.
- [6] Cihang Xie, Zhishuai Zhang, Yuyin Zhou, Song Bai, Jianyu Wang, Zhou Ren, and Alan L Yuille, “Improving transferability of adversarial examples with input diversity,” in *Proceedings of the IEEE/CVF conference on computer vision and pattern recognition*, 2019, pp. 2730–2739.
- [7] Xiaosen Wang and Kun He, “Enhancing the transferability of adversarial attacks through variance tuning,” in *Proceedings of the IEEE/CVF Conference on Computer Vision and Pattern Recognition*, 2021, pp. 1924–1933.
- [8] Yifeng Xiong, Jiadong Lin, Min Zhang, John E Hopcroft, and Kun He, “Stochastic variance reduced ensemble adversarial attack for boosting the adversarial transferability,” in *Proceedings of the IEEE/CVF Conference on Computer Vision and Pattern Recognition*, 2022, pp. 14983–14992.
- [9] Huanran Chen, Yichi Zhang, Yinpeng Dong, and Jun Zhu, “Rethinking model ensemble in transfer-based adversarial attacks,” *arXiv preprint arXiv:2303.09105*, 2023.
- [10] Jiadong Lin, Chuanbiao Song, Kun He, Liwei Wang, and John E Hopcroft, “Nesterov accelerated gradient and scale invariance for adversarial attacks,” *arXiv preprint arXiv:1908.06281*, 2019.
- [11] Hao Huang, Ziyang Chen, Huanran Chen, Yongtao Wang, and Kevin Zhang, “T-sea: Transfer-based self-ensemble attack on object detection,” in *Proceedings of the IEEE/CVF Conference on Computer Vision and Pattern Recognition*, 2023, pp. 20514–20523.
- [12] Kenji Kawaguchi, Jiaoyang Huang, and Leslie Pack Kaelbling, “Every local minimum value is the global minimum value of induced model in nonconvex machine learning,” *Neural Computation*, pp. 2293–2323, 2019.
- [13] Thomas Laurent and James Brecht, “Deep linear networks with arbitrary loss: All local minima are global,” in *International conference on machine learning*, 2018, pp. 2902–2907.
- [14] Huanran Chen, Shitong Shao, Ziyi Wang, Zirui Shang, Jin Chen, Xiaofeng Ji, and Xinxiao Wu, “Bootstrap generalization ability from loss landscape perspective,” in *European Conference on Computer Vision*, 2022, pp. 500–517.
- [15] Zeming Wei, Jingyu Zhu, and Yihao Zhang, “On the relation between sharpness-aware minimization and adversarial robustness,” *arXiv preprint arXiv:2305.05392*, 2023.
- [16] Zeming Wei, Yifei Wang, Yiwen Guo, and Yisen Wang, “Cfa: Class-wise calibrated fair adversarial training,” in *Proceedings of the IEEE/CVF Conference on Computer Vision and Pattern Recognition*, 2023, pp. 8193–8201.
- [17] Sébastien Marcel and Yann Rodriguez, “Torchvision the machine-vision package of torch,” in *Proceedings of the 18th ACM international conference on Multimedia*, 2010, pp. 1485–1488.
- [18] Hadi Salman, Andrew Ilyas, Logan Engstrom, Ashish Kapoor, and Aleksander Madry, “Do adversarially robust imagenet models transfer better?,” *Advances in Neural Information Processing Systems*, pp. 3533–3545, 2020.
- [19] Edoardo Debenedetti, Vikash Sehwal, and Prateek Mittal, “A light recipe to train robust vision transformers,” in *2023 IEEE Conference on Secure and Trustworthy Machine Learning (SaTML)*, 2023, pp. 225–253.
- [20] Francesco Croce, Maksym Andriushchenko, Vikash Sehwal, Edoardo Debenedetti, Nicolas Flammarion, Mung Chiang, Prateek Mittal, and Matthias Hein, “Robustbench: a standardized adversarial robustness benchmark,” *arXiv preprint arXiv:2010.09670*, 2020.
- [21] Jiakai Wang, “Adversarial examples in physical world,” in *IJCAI*, 2021, pp. 4925–4926.